

An experimental study on the performance of proton exchange membrane fuel cell

M. KELLEGOZ*, I. OZKAN

Eskisehir Osmangazi University, Physics Department, 26480 Eskisehir, Turkey

It is known that different operating conditions influence the performance of the proton exchange membrane fuel cell. The effects of different humidification temperatures, backpressures, and flow rates of the reactant gases on the performance of the proton exchange membrane fuel cell have been studied experimentally. Results are presented in the form of I-V polarization curves. The possible mechanisms and their interrelationships for these results are discussed. Commonly it can be said that the electrochemical reaction rate have to be controlled at its maximum rate. Because, excessive use of required operating conditions cause "flooding" this in turn decreases the electrochemical reaction. In this context, the optimum working conditions under the cell temperature of 70°C were found to be as follows: anode humidification temperature of 75°C; cathode humidification temperature of 90°C; backpressures of 3atm on both sides, and flow rates of 40cm³/min on both sides. Under these conditions, the amount of the maximum power density was determined as 0.727 W/cm².

(Received December 01, 2014; accepted April 05, 2016)

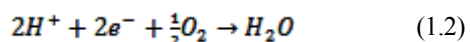
Keywords: Proton exchange membrane fuel cell, Performance test, Polarization curves, Operating conditions

1. Introduction

Most energy systems that mankind use provides their energy requirements from fossil originated fuel sources. Because of the negative environmental effects and increasingly depletion of these traditional fuel sources, studies directed to clean and renewable energy sources that can be substituted for fossil originated fuels and technologies [1]. Proton exchange membrane fuel cell(PEMFC) has received much attention in the last few decades according to other kinds of fuel cells because of its high efficiency, durability, lightweight, compactness, harmless and usage as energy converter in fixed and mobile applications [2-8]. A typical PEMFC structure consists of two electrodes as an anode and a cathode which are separated by a proton exchange membrane (PEM) that acts as an electrolyte. Hydrogen gas (H₂) that is used as fuel flows through a network of channels to the anode, where it separated into protons and electrons. While protons flow through the PEM, electrons flow over an external load (R_L) to the cathode. Electrons that flow over R_L produce an electric current from the PEMFC. Oxygen gas (O₂) that is used as oxidant flows through a similar network of channels to the cathode, where it combines with protons and electrons to form water (H₂O). The reaction for H₂O formation is an exothermic reaction. Therefore heat is produced beside H₂O. The reactions on the anode and cathode sides are



and



respectively. The total reaction is given as



Thus a PEMFC is an electrochemical device that converts energy into electrical energy by a chain of reactions [1-2,9]. When R_L is kept wide, a performance curve can be obtained which is useful in the explanation of physical and chemical relationships, and the fundamental operating principles of PEMFC. The current and voltage values of the obtained performance curve depend on both the electrochemical reactions on the anode and cathode of the PEMFC and R_L [10-11]. The performance of PEMFC is known to be influenced by different operating conditions like pressure, temperature and humidification of the reactant gases. Many studies [12-20] have been done in order to understand and improve the performance of PEMFC.

In this work, an experimental study has been done to understand the performance of PEMFC under different humidification temperatures, backpressures, and flow rates of the reactant gases. This was illustrated by using a double cell stack home-made PEMFC.

2. Experimental

2.1 Preparation of PEM

Commercially obtained NRE-212 Nafion® membrane was used to prepare the required PEM having 0.05mm thickness and 36cm² surfaces. PEM has been purified from surface, organic and metal ion contaminations. This process has been done by boiling the membrane for 75min at 80°C, in pure water, 15% hydrogen peroxide solution and 50% sulfuric acid solution, respectively. Finally PEM

was purified from sulfuric acid solution by double rinsing in pure water for 15min at 80°C. Water bath was used for heating the PEMs which was immersed in beakers of the relevant solutions. Finally, PEM was stored in pure water to avoid it from environmental pollutions.

2.2 Preparation of electrodes and gas diffusion layers(GDLs)

Commercially obtained CC-S type carbon cloths were used as electrodes and GDLs. Only one side of the electrodes was loaded with 0.5mg/cm² platinum (Pt) as catalyst. Catalyzing solution was used for loading the electrodes with Pt. The solution was prepared by using Ammonium Ferric (III) oxalate and Potassium Tetrachloroplatinate (II) chemicals. Brush method was used for applying the prepared solution onto the electrodes. The covered electrodes were dried overnight at room temperature.

2.3 Preparation of membrane-electrode assembly (MEA)

MEA is the heart of PEMFC. It consists of a PEM and two electrodes bounded on each side of the PEM by a commercially obtained 5% w/w Perfluorosulfonic acid solution. The electrodes with the Pt loaded side having 16cm² surface were placed in the middle of the each side of PEM having 36cm² surface. Hot pressing has been performed at 130°C and 250psi for 5 min to obtain MEA.

2.4 Preparation of gas flow plates and gas flow channels

Commercially obtained graphite plates were used as gas flow plates. Graphite plates are well machinable materials. A graphite plate with the dimension of

6x6x1.5cm (LxWxH) and two graphite plates with the dimension of 6x6x1cm (LxWxH) were used as gas flow plates. Gas flow channels were drilled on the surfaces of them. Vertical straight configuration was used as gas flow channels as shown in Fig. 1.

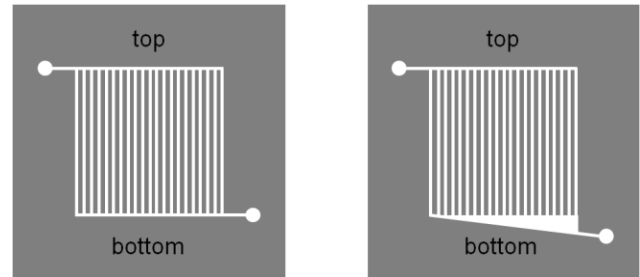


Fig. 1. Vertical straight configured gas flow channels

The widths of both the gas flow channel and rib are 1mm. In this case the active gas flow area ratio is 45.13%. Each gas flow field consists of 21 vertical straight parallel gas flow channels and 19 ribs. The slope at the bottom of the gas flow field provides better flow and drip of water. While the two graphite plates with the sloped gas flow field were used on the cathode side, the graphite plate without slope was used on the anode side.

2.5 Assembly of PEMFC

The double cell stack PEMFC was assembled with MEA, gas flow plates, current collector strips, convenient gaskets which are kept together with screws and nuts by using end plates. A schematic drawing of the double cell stack PEMFC is shown in Fig. 2.

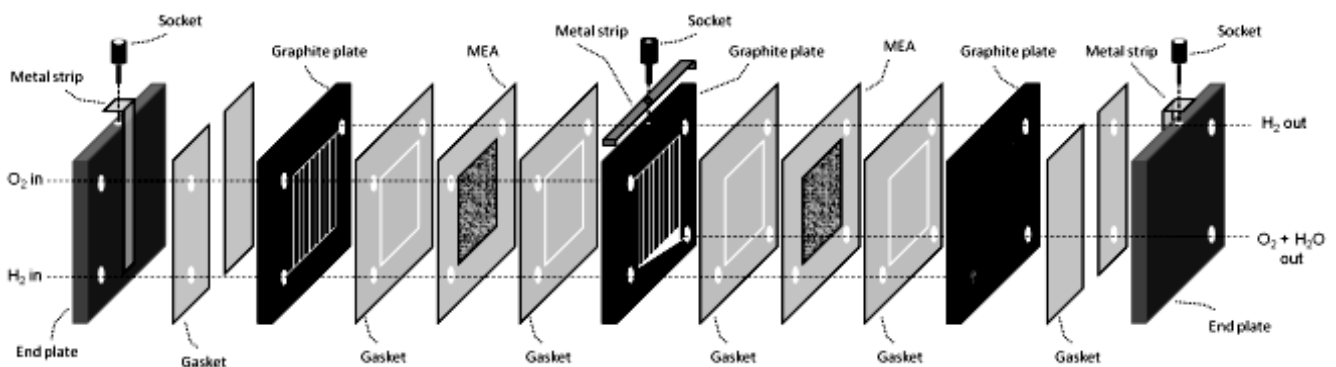


Fig.2. Schematic drawing of double cell stack PEMFC.

2.6 Experimental setup

A schematic diagram of the experimental setup employed in this paper is shown in Fig. 3. This setup consists of seven major units, i.e., gas supply unit, humidifying (HMD) unit, flow rate control (FM) unit,

pressure (P) and temperature (T) measurement unit, water collecting (WCT) unit, pressure control unit and electric test unit.

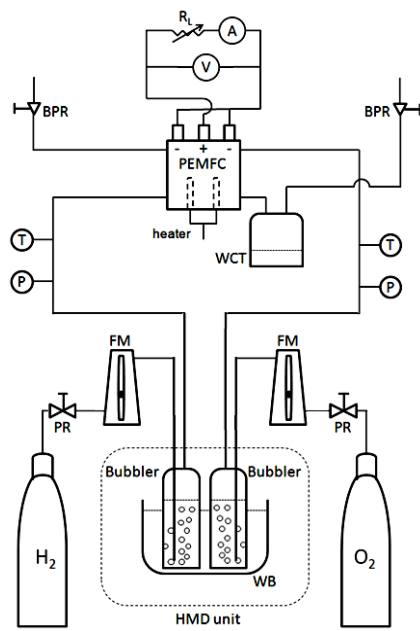


Fig. 3. Experimental setup diagram.

The gas supply unit supplies the reactant gases as H₂ and O₂ for the PEMFC. The HMD unit provides the humidification of inlet reactant gases. Besides it also provides heating of the gases via adjusting the temperature by water bath (WB). The FM unit controls the rate of the inlet gases that feed the PEMFC. The P and T measurement units were used for measuring the pressure

and temperature of the inlet gases just before the PEMFC. The WCT unit collects water that occurs during the reaction on the cathode sides of PEMFC. The pressure control unit which consists of a pressure regulator was used to control the pressure of the gases from the supply unit. Besides, with the addition of a back pressure regulator (BPR), pressure control unit allowed to keep the pressures of the reactant gases at a constant value. The electric test unit was used to obtain the electrical performance as I-V characteristics.

2.7 PEMFC tests

Different operating conditions were applied to determine the performance of the PEMFC. The conditions were obtained by varying the pressure, temperature, humidity and flow rate of the reactant gases to determine the effects of them on the performance of the PEMFC. The operating conditions and experimental parameters can be seen in detail in Table 1. The PEMFC was operated overnight before evaluating the I-V characteristics for each set. Every best result of each set was used in the next set of experiments so that we can reach to the optimum operating condition of the PEMFC at last. The measurements were performed by using a voltmeter and an ammeter and by varying the R_L. These measurement results were used to plot the performance curve to determine the I-V characteristics of the PEMFC at the relevant operating conditions.

Table 1. Operating conditions and experimental parameters.

Set	1	2	3	4
Common operating conditions	PH ₂ :2atm; PO ₂ :2atm TH ₂ :70°C; TO ₂ :70°C Flow rate H ₂ :40cm ³ /min; Flow rate O ₂ :40cm ³ /min	HMDH ₂ :+; HMDO ₂ :+ (² opt) PH ₂ :2atm; PO ₂ :2atm Flow rate H ₂ :40cm ³ /min; Flow rate O ₂ :40cm ³ /min	HMDH ₂ :+; HMDO ₂ :+ (opt) TH ₂ :75°C; TO ₂ :90°C (opt) Flow rate H ₂ :40cm ³ /min; Flow rate O ₂ :40cm ³ /min	HMDH ₂ :+; HMDO ₂ :+ (opt) TH ₂ :75°C; TO ₂ :90°C (opt) PH ₂ :3atm; PO ₂ :3atm (opt)
Variable	¹ Humidity	Temperature (°C)	Pressure (atm)	Flow rate (cm ³ /min)
Experiment 1	H ₂ : + O ₂ : +	H ₂ : 70, 75, 80, 85, 90 O ₂ : 70, 70, 70, 70, 70	H ₂ : 1, 2, 3, 4 O ₂ : 1, 1, 1, 1	H ₂ : 10, 20, 30, 40 O ₂ : 40, 40, 40, 40
Experiment 2	H ₂ : - O ₂ : +	H ₂ : 70, 70, 70, 70, 70 O ₂ : 70, 75, 80, 85, 90	H ₂ : 1, 1, 1, 1 O ₂ : 1, 2, 3, 4	H ₂ : 40, 40, 40, 40 O ₂ : 10, 20, 30, 40
Experiment 3	H ₂ : + O ₂ : -	H ₂ : 70, 75, 80, 85, 90 O ₂ : 70, 75, 80, 85, 90	H ₂ : 1, 2, 3, 4 O ₂ : 1, 2, 3, 4	H ₂ : 10, 20, 30, 40 O ₂ : 10, 20, 30, 40
	¹ + (humidified); - (non-humidified)			
	² optimum			

3. Results and discussion

3.1 Effects of humidification

Three experiments of set 1 were carried out to study the effects of humidification of the reactant gases on the

performance of the PEMFC. First experiment was performed by using humidified reactant gases on both the anode and the cathode sides. Second experiment was performed by humidified O₂ on the cathode side while H₂ on the anode side was kept in a non-humidified condition. In the third experiment humidified H₂ was used on the

anode side while O_2 on the cathode side was non-humidified. The humidification process was done by using water bath and bubblers. During these experiments backpressures, temperatures and flow rates of the reactant gases were constant at 2atm, $70^\circ C$ and $40\text{cm}^3/\text{min}$, respectively. PEMFC temperature was maintained at $70^\circ C$.

In Fig.4, performance curves with the above mentioned humidification conditions on both the anode and the cathode sides are presented. The performance curve with humidified reactant gases shows the best performance. The performance decreases with the usage of non-humidified reactant gases. The decrease in performance with the non-humidified anode side was higher than the non-humidified cathode side. In all three experiments it can be seen that especially the reactant gas of the anode side have to be humidified for a good performance. This observation can be explained with the results of Nguyen et.al. [21] who found that at high current densities ohmic losses in the PEM accounts for a large friction of the voltage loss in the PEMFC and back diffusion of H_2O from the cathode side of the PEM is insufficient to keep the PEM hydrated for well conductivity. Therefore to minimize the ohmic loss the reactant gas of the anode side has to be humidified. The appropriate humidification temperatures of the reactant gases are discussed in the next section.

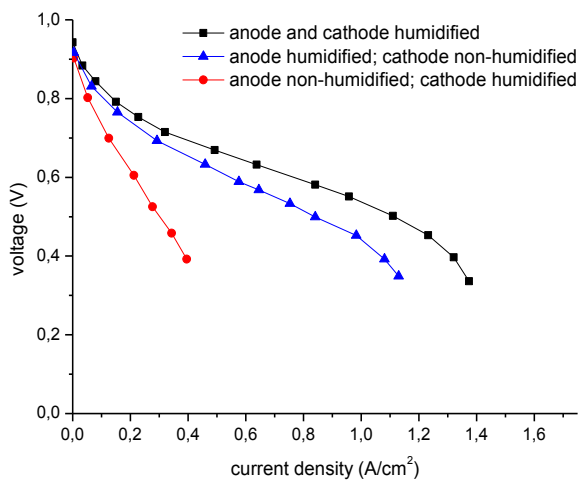


Fig. 4. Performance curves for various humidification conditions.

3.2 Effects of humidification temperatures

Three experiments of set 2 were carried out to study the effects of humidification temperatures of the reactant gases on the performance of the PEMFC. In the first experiment, the cathode humidification temperature was maintained at $70^\circ C$ while the anode humidification temperature was changed from 70 to $90^\circ C$ by $5^\circ C$ steps. Second experiment was performed by increasing the cathode humidification temperature from 70 to $90^\circ C$ by $5^\circ C$ steps whereas the anode humidification temperature

was maintained at $70^\circ C$. Third experiment was performed by increasing the humidification temperatures from 70 to $90^\circ C$ by $5^\circ C$ steps on both sides of the electrodes. These processes were done by heating the relevant reactant gases. During these experiments, backpressures and flow rates of the reactant gases were constant at 2atm and $40\text{cm}^3/\text{min}$, respectively. The best humidification condition on section 3.1 was applied in this set of experiments. PEMFC temperature was kept at $70^\circ C$.

In Fig.5, performance curves of various anode humidification temperatures are presented. The PEMFC performance was improved with the increase of the anode humidification temperature from 70 to $75^\circ C$. Performance begins to decrease slightly from 75 to $80^\circ C$. A drastic decrease can be seen between 80 and $90^\circ C$. These results can be explained as follows: Performance increment from 70 to $75^\circ C$ can be explained by the increase in the conductivity of the PEM at high temperatures which was also concluded by Sone et al. [22], Ozen et al. [23] and Kadjo et al. [24]. The increase in the diffusivity of the reactant gases with the increase of the temperatures is also effective on the performance. The performance loss after a critical temperature ($80^\circ C$) can be explained by the reduction of the active surface area with the increase of the H_2O amount that produced by the electrochemical reaction on the cathode side. This phenomenon caused by the H_2O flooding on the cathode side that reduces the reaction rate so that the current decreases to a lower level as concluded by Voss et al. [25].

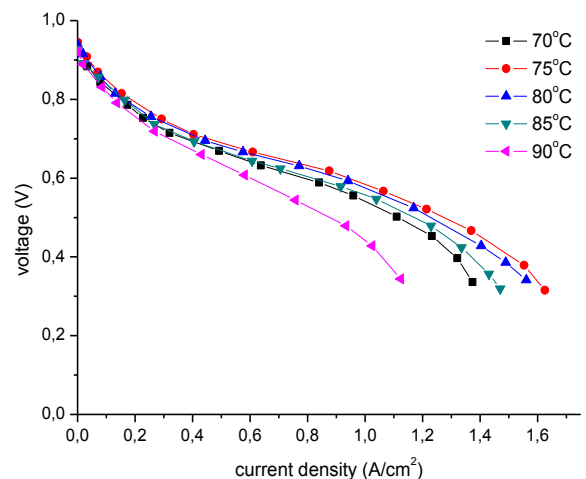


Fig. 5. Performance curves for various anode humidification temperatures.

In Fig.6 performance curves of various cathode humidification temperatures are presented. The performance was improved with the increase of the cathode humidification temperatures which were chosen from 70 to $90^\circ C$. All performance curves are rather closed to each other. The slight increase in the performance of the PEMFC with the increase of the cathode humidification temperatures from 70 to $90^\circ C$ can be explained by the

different H_2O concentration gradient between the anode and the cathode. The H_2O concentration of the cathode side rises with the increase of the cathode humidification temperature. In this state back diffusion process occurs and H_2O migrates from the cathode side to the anode side through the PEM. This phenomenon contributes to the anode humidification by increasing it a little more. As seen in Fig. 5, performance increases with the increase of the anode humidification temperature from 70 to 75°C. Besides this explanation the increase in the hydration of the PEM is also effective in this occurrence, which cause an increase in the conductivity so that the current increases to a higher level slightly as concluded by Sone et al. [22].

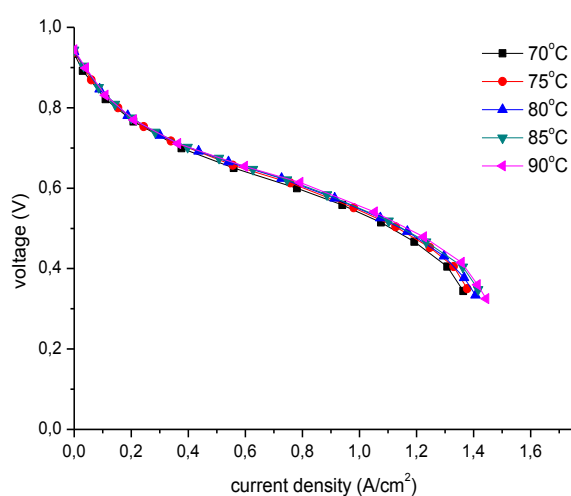


Fig. 6. Performance curves for various cathode humidification temperatures.

In Fig. 7, performance curves of various humidification temperatures are presented. The humidification temperatures are equal to each other and were changed from 70 to 90°C by 5°C steps. The performance was improved with the increase of the humidification temperature from 70 to 75°C on both side of the electrodes. There is no apparent change in the performance of the PEMFC with the change in the humidification temperature from 75 to 80°C. Performance begins to decrease from 80 to 90°C. These results can be explained by the change in the conductivity and hydration of the PEM as concluded by Kordesch et al. [7] and Wintersgill et al. [26]. It is also explained by the further accumulation of H_2O on the cathode side. The reason of the increase in the performance between 70 and 75°C is the increase in the conductivity at high temperatures. However, the increase in the diffusivity of the reactant gases is also effective. The decrease in the performance between 80 and 90°C causes by the H_2O flooding on the cathode side that reduces the reaction rate. Thus the performance decreases despite the increase of the humidification temperatures of the reactant gases.

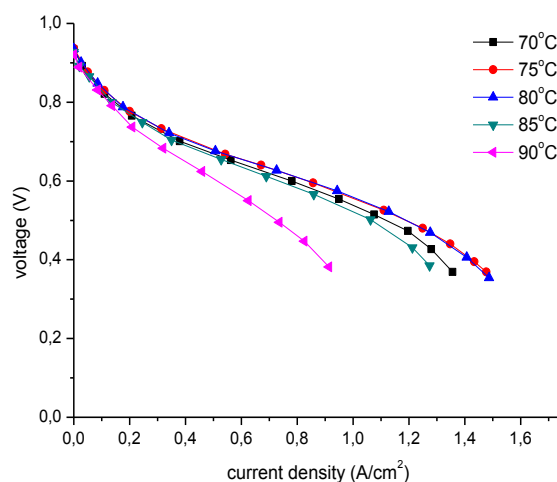


Fig. 7. Performance curves for various humidification temperatures. ($T_{anode} = T_{cathode}$).

3.3 Effects of backpressures

Three experiments of set 3 were carried out to study the effects of backpressures of the reactant gases on the performance of the PEMFC. First experiment was performed by increasing of the backpressure on the anode side from 1 to 4atm by 1atm steps, whereas the backpressure on the cathode side maintained at 1atm. Second experiment was performed by the increase of the backpressure on the cathode side from 1 to 4atm by 1atm steps, whereas the backpressure on the anode side maintained at 1atm. In the third experiment the backpressures on both the anode and the cathode sides were increased from 1 to 4atm by 1atm steps. During these experiments flow rates of the reactant gases were constant at 40cm³/min. The best humidification condition (anode and cathode humidified) on section 3.1 and the best humidification temperatures (anode humidification temperature was 75°C; cathode humidification temperature was 90°C) on section 3.2 were applied in this set of experiments. PEMFC temperature was maintained at 70°C.

In Figs. 8 and 9, performance curves of various anode and cathode backpressures are presented, respectively. The PEMFC performance was improved with the increase of the relevant backpressures from 1 to 4atm. A notable improvement was observed due to the pressurized cathode side rather than the pressurized anode side. The increase in the electrochemical reaction rate on the cathode side has more effect than that of the anode side on the performance of the PEMFC. The open circuit voltage increases with the increase in backpressure. These results can be explained by the increase in the partial pressure of the reactant gases according to the Nernst equation [27].

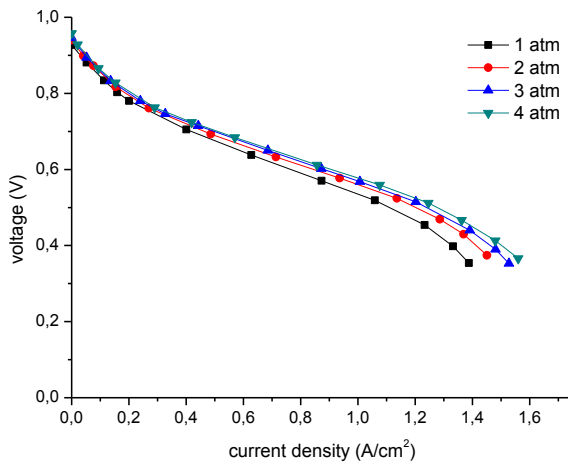


Fig. 8. Performance curves for various anode backpressures.

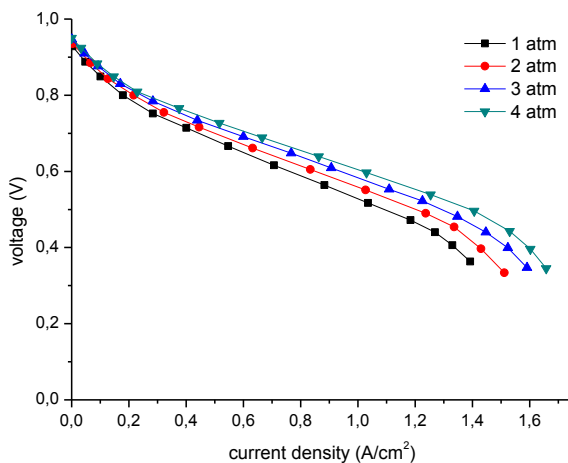


Fig. 9. Performance curves for various cathode backpressures.

In Fig. 10, performance curves of various backpressures are presented. The backpressures are equal to each other and were varied from 1 to 4 atm by 1 atm steps. The open circuit voltage increases with the increase in backpressure. Performance begins to increase from 1 to 3 atm. A decrease can be seen between 3 and 4 atm. These results can be explained as follows. Performance increment from 1 to 3 atm can be explained by the increase in the partial pressure of the reactant gases. The density and diffusivity of the reactant gases are also effective on the performance. Even if the humidification temperatures are equal to each other at different backpressures, the humidified reactant gas density hydrates the PEM at higher backpressures more easily. This causes the electrochemical reaction rates to rise. The performance loss between 3 and 4 atm can be explained by the reduction of the active surface area with the increase of the H_2O amount that produced by the electrochemical reaction

on the cathode side. This phenomenon caused to H_2O flooding on the cathode side that reduce the reaction rate so that the current decrease to a lower level.

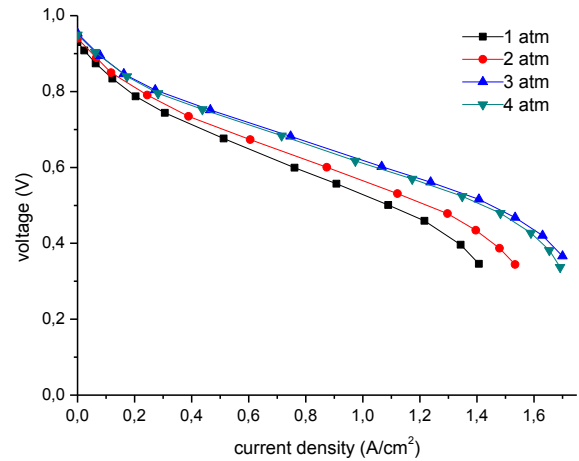


Fig. 10. Performance curves for various backpressures.

3.4 Effects of reactant gas flow rates

Two experiments of set 4 were carried out to study the effects of flow rates of the reactant gases on the PEMFC. First experiment was performed by the increase of the flow rate on the anode side from 10 to $40\text{cm}^3/\text{min}$ by $10\text{cm}^3/\text{min}$ steps, whereas the flow rate on the cathode side maintained at $40\text{cm}^3/\text{min}$. Second experiment was performed by the increase of the flow rate on the cathode side from 10 to $40\text{cm}^3/\text{min}$ by $10\text{cm}^3/\text{min}$ steps, whereas the flow rate on the anode side maintained at $40\text{cm}^3/\text{min}$. During these experiments the best conditions (anode and cathode humidified; anode humidification temperature was 75°C , cathode humidification temperature was 90°C ; anode and cathode backpressures were 3 atm each) on section 3.1, 3.2 and 3.3 were applied in this set of experiments. PEMFC temperature was maintained at 70°C .

In Fig. 11, performance curves of various anode and cathode flow rates are presented, respectively. The performance curves have no significant difference. The curves were nearly congruent to each other despite the change of the anode flow rate from 10 to $40\text{cm}^3/\text{min}$. This can be explained by the limited electrochemical reaction rate on the cathode side as concluded by Wang et al. [28] and Dietmar et al. [29] which has a fixed flow rate of $40\text{cm}^3/\text{min}$. On the other hand an increase can be seen on the performance of the PEMFC by changing the cathode flow rate from 10 to $40\text{cm}^3/\text{min}$ by $10\text{cm}^3/\text{min}$ steps, whereas the anode flow rate was fixed to $40\text{cm}^3/\text{min}$. This phenomenon can be explained by the decrease of the electrochemical reaction rate on the cathode side in which the oxidant amount is reduced step by step as concluded by Sreenivasulu et al. [30].

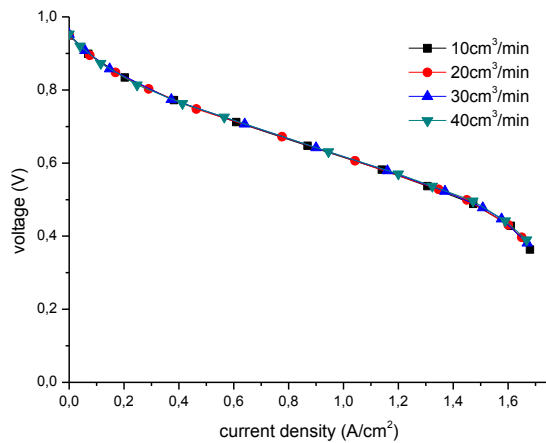


Fig. 11. Performance curves for various flow rates.

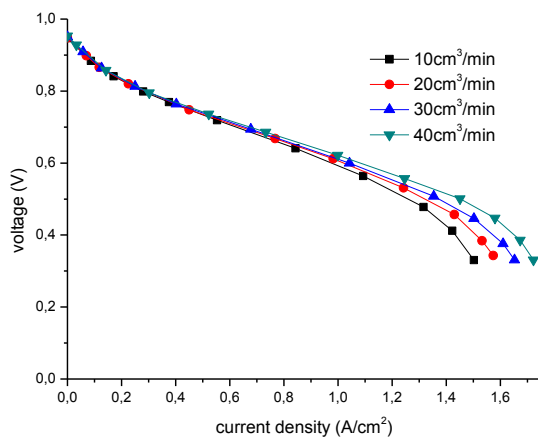


Fig. 12. Performance curves for various flow rates.

The polarization and power density curves are given in Fig. 13. It can be seen that the best power density is determined at $0.727\text{W}/\text{cm}^2$.

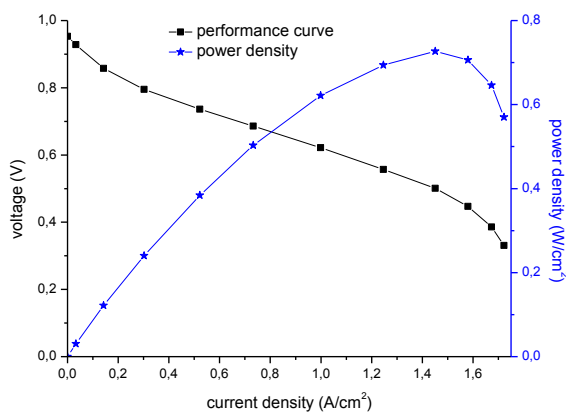


Fig. 13. Maximum performance and power density curves.

4. Conclusions

In this work, a double cell stack home-made PEMFC having H_2/O_2 feeding was designed and effects of the operating conditions on its performance was investigated. The performance of the PEMFC was strongly dependent on the humidification, backpressure, and gas flow rate of the reactant gases. The experiments were performed by changing these operating conditions.

Humidified reactant gases improve the performance of the PEMFC. This is related to the increasing conductivity of PEM which resulted from the hydration. If the provided humidification is insufficient, the performance of the PEMFC became worse. Commonly the increase of the humidification temperature, backpressure, and flow rate of the reactant gases improves the performance of the PEMFC. But, above the critical values of the operating conditions the performance decreases.

The anode humidification temperature has significant effects on the performance of the PEMFC. Above a critical humidification temperature of the anode side the performance decreased due to the “flooding” on the cathode side by the further accumulated H_2O that reduced the active reaction area. The cathode humidification temperature has no significant effects on the performance of the PEMFC. The increase in the backpressure of the anode and cathode side separately improves the performance of the PEMFC. The pressurized cathode side has attractive effects on the performance of the PEMFC than the pressurized anode side. When both the anode and the cathode backpressures increased synchronously, the performance of the PEMFC improves until a critical backpressure. Above the relevant backpressure the performance decreased due to the partial pressures of the reactant gases. The anode flow rate has no significant effects on the performance of the PEMFC. Performance curves are nearly congruent to each other. The decrease in the flow rate of the cathode side reduces the performance of the PEMFC due to the reduction of the oxidant.

The optimum conditions in this work are obtained at 3atm on both side of the electrodes, 70°C at anode humidification temperature, 90°C at cathode humidification temperature, and $40\text{cm}^3/\text{min}$ of flow rate on both side of the electrodes under the cell temperature at 70°C . Under these conditions, maximum power density was determined at $0.727\text{W}/\text{cm}^2$.

Acknowledgements

A part of this work has been financed and supported by the scientific research commission of Eskisehir Osmangazi University of Turkey with the project number of 200319010 and 201215015.

References

- [1] H.T. Liu, F. Barbir, A. Kazim, S. Kakaç, Fuel Cells - The clean energy converter. Proceedings of the First Trabzon International Energy and Environmental Symposium, Karadeniz Technical University, Trabzon, Turkey. p.3,1996.
- [2] F. Barbir, T. Gomez, Int. J. Hydrogen Energy, **22**, 1027 (1997).
- [3] K. Kinoshita, E. R. McLarnon, E. J. Cairns, Fuel Cells - A Handbook, (1988).
- [4] K. B Prater. J. Power Sources, **61**, 105 (1996).
- [5] Z. Qi, A. Kaufmann, J. Power Sources, **113**, 37 (2003).
- [6] J. Larminie, A. Dicks, Fuel Cell Systems Explained, New York:Wiley 2000.
- [7] K. Kordesch, G. Simader, Fuel Cells and Their Applications. Weinheim:Wiley, 1996.
- [8] P. Costamagna, S. Srinivasan, J. Power Sources,**102**, 242 (2001).
- [9] J. B. Benzinger, M. B. Satterfield, W.H.J. Hogarth, J.P. Nehlsen, I.G. Kevrekidis, Power Sourcesm,**155**, 272 (2005).
- [10] EG&G Services, I. Parson, Fuel Cell Handbook. Morgantown/WV: U.S. Department of Energy, p. 3.1, 2000.
- [11] A. Rowe, X. Li, J. Power Sources,**102**, 82 (2001).
- [12] Y.M. Ferng, Y.C. Tzang, B.S. Pei, C.C. Sun, A. Su, J. Hydrogen Energy, **29**, 381 (2004).
- [13] L. Wang, A. Husar, T. Zhou, H. A. Liu, Int. J. Hydrogen Energy **28**, 1263 (2008).
- [14] D. Hyun, J. Kim, J. Power Sources,**126**, 98 (2004).
- [15] J.J. Hwang, J. Power Sources,**104**, 24 (2002).
- [16] A. Kazim, P. Forges, H.T. Liu, Int. J. Energy Resources, **27**, 401 (2003).
- [17] Q. Yan, H. Taghiani, H. Causey, J. Power Sources, **161**, 492 (2006).
- [18] M. Amirinejad, S. Rowshanzamir, M.H. Eikani, J. Power Sources, **161**, 872 (2006).
- [19] M. Kellegöz, Different type of proton exchange membrane fuel cell design and measurements. Turkey:Eskisehir Osmangazi University;(2005).
- [20] M. Kellegöz, I. Özkan, M.S. Kılıçkaya, J. Optoelectron. Adv. Mat.**10**, 369 (2008).
- [21] T.V. Nguyen, R.E. White, J. Electrochem. Soc. **140**(8), 178 (1993).
- [22] Y. Sone, P. Ekdunge, D. Simonsson, J. Electrochem. Soc.**143**, 1254 (1996).
- [23] D.N. Ozen, P. Timurkutluk, K. Altinisik. Renewable and Sustainable Energy Reviews, **59**, 1298 (2016).
- [24] A.J.J. Kadjo, P. Brault, A. Caillard, C. Countanceau, J.P. Gamier, S. Martemianov, J. Power Sources,**172**, 613 (2007).
- [25] H.H. Voss, D.P. Wilkinson, P.G. Pickup, M.C. Johnson, V. Basura, Electrochem. Acta, **40**, 321 (1995).
- [26] M.C. Wintersgill, J.J. Fontanella, Electrochem. Acta, **143**, 1533 (1998).
- [27] S.J. Cheng, J.M. Miao, S.J. Wu, Renewable Energy, **39**, 250 (2012).
- [28] L. Wang, H. Liu, J. Power Sources, **134**, 185 (2004).
- [29] G. Dietmar, Z. Nada, S. Christian, G. Florian, L. Victor, H. Christopher, Int. J. Hydrogen Energy, **37**, 7736 (2012).
- [30] B. Screenivasulu, G. Vasu, V. Dharma, S.V. Naiolu, Int. J. Hydrogen Energy, **2**, 291 (2012).

*Corresponding author: murke@ogu.edu.tr